Additive Manufacturing 23 (2018) 287–293

Contents lists available at ScienceDirect

Additive Manufacturing

journal homepage: www.elsevier.com/locate/addma

Full Length Article

Micro-scale finishing of the surface and form of a Ti-6Al-4V lightweight rotor obtained by laser powder bed fusion used for air bearing

Claude Sanz[a,b,*], Romain Gerard[b], Paul Morantz[c,d], Ahmed Chérif[b], Paul Shore[c,d], Hélène Mainaud-Durand[b], Alexander J.G. Lunt[b]

[a] Cranfield University, College Rd, Cranfield MK43 0AL, UK
[b] CERN, 385 Route de Meyrin, 1217, Meyrin, GE, CH, Switzerland
[c] Loxham Precision, College Rd, Cranfield MK43 0AL, UK
[d] National Physical Laboratory, Hampton Road, Teddington, Middlesex, TW11 0LW, UK

ARTICLE INFO

Keywords:
Precision machining
Microscale tolerances
Residual stress
Selective laser melting
Lightweight air bearing

ABSTRACT

The European Organisation for Nuclear Research, CERN, is in the process of designing and testing parts for the next generation of linear accelerators. In order to operate the experiments, the pre-alignment precision of the components of the two opposing accelerating complexes has placed increased demands on part tolerances, which are now approaching the micrometre. In order to meet these demanding requirements, improvements are necessary to the build processes, machining parameters and post-manufacture characterisation stages. One of the most promising methods for the production of these parts is Laser Powder Bed Fusion, and as such, this paper focuses on the manufacture of the lightweight air bearing rotor component and the micro-scale tolerance machining required by this part. The results demonstrate that despite being able to initially machine the part to a form tolerance approaching 2 µm, subsequent notch cutting and the release of residual stresses from the part obtained by Laser Powder Bed Fusion induces an 18 µm part misalignment which is larger than the tolerance limits of 5 µm required for operation. This demonstrates that further minimisation and understanding of the residual stresses induced during machining are required to facilitate the effective manufacture of high precision components of this type.

1. Introduction

Additive manufacturing [1] is used in many fields: for instance, it allows fast prototyping and art designers to express their ideas in three dimensions and it improves the characteristics of some technical parts. Nonetheless, high precision mechanics applications using additive manufacturing are less common. As a matter of facts, the distortions introduced during the part's additive manufacture and the difficulties encountered during machining, including stresses management, repel precision engineers. These are subjects discussed in this manuscript, which focuses on the example of a rotor produced by Laser Powder Bed Fusion, known as Selective Laser Melting (SLM).

The European Organisation for Nuclear Research (CERN) designs and develops the next generation of research facilities. Among them is the Compact LInear Collider (CLIC): a 48 km long linear collider capable of accelerating two beams of electrons or positrons in two opposing directions with a focal ellipse size of 1 nm × 40 nm. A major challenge within this project is the pre-alignment of the thousands of accelerator components in order to ensure that the beam passes through the collider unimpeded on start-up. For example, quadrupole magnets have an alignment budget of error of 14 µm which needs to be maintained over a distance of 200 m along the length of the accelerator [2].

The state-of-the-art alignment techniques are only able to meet tolerances greater than 20 µm. For this reason, a consortium of researchers: CERN personnel, European academies and leading industrial partners has been assembled to work together in the PACMAN (Particle Accelerator Component's Metrology and Alignment to the Nanometre scale) project [3]. One goal of this taskforce is to carefully materialise the functional axis of the CLIC accelerator elements and determine its position with respect to external references called fiducials [4]. The first step is performed without the presence of the beam. It involves identifying the beam axis within the magnet using a conductive stretched

* Corresponding author at: Route de Divonne 12, 1291, Commugny, VD, Switzerland.
E-mail addresses: MsClaudeSanz@gmail.com (C. Sanz), Romain.Gerard@CERN.ch (R. Gerard), Paul.Morantz@LoxhamPrecision.com (P. Morantz), Ahmed.Cherif@CERN.ch (A. Chérif), Paul.Shore@NPL.co.uk (P. Shore), Helene.Mainaud.Durand@CERN.ch (H. Mainaud-Durand), Alexander.Lunt@CERN.ch (A.J.G. Lunt).

https://doi.org/10.1016/j.addma.2018.05.033
Received 26 March 2018; Received in revised form 14 May 2018; Accepted 17 May 2018
Available online 26 July 2018

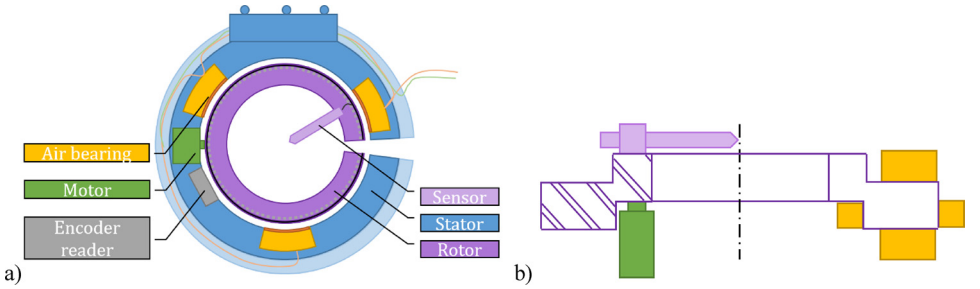

Fig. 1. a) Schematic of the SESHAT design concept b) Technical drawing extract of an alumina version of SESHAT's rotor (in purple) with its rotational axis – aligned with the wire during the measurement (in dashed black), the arrangement of the sensor attached to the rotor (in pink), the arrangement of 4 air pads (in yellow) and the actual orientation of the piezo motor (in green).

wire [5,6] which then provides a physical representation of the beam axis. The wire location can finally be measured using a Coordinate Measurement Machine (CMM) in order to determine the relative beam position with sub-micron accuracy.

A review of the characteristics of suitable wires for this application recently concluded that the largest source of uncertainty in the measurement approach is associated with wire form errors. Further, it concluded that existing metrology technologies are unable to measure the roundness of a wire to the precision required for the CLIC project. For this reason, a new measurement device, known as the Shape Evaluating Sensor: High Accuracy and Touchless (SESHAT), is under development. The stretched wire position forms a reference for machine alignment, and therefore the wire cannot be touched during measurement. This results in one of the most unusual features of the SESHAT: an open notch required on one side so that the stretched wire can be passed through the air bearing stator and rotor in order to reach the measurement area. It appears in Fig. 1.

In order to enable the effective movement around the wire, the bearings between the stator and rotor are required to be stiff and to function effectively despite the hole in the rotor's bearing surface. For this reason, flat, radial convex and concave NewWay porous air pads, have been selected. These pads operate by expelling compressed air from the entire bearing surface. The high stiffness and low random error motion of this type of bearing are dependent on the quality and alignment of the bearing surfaces. As a result, the tolerances on the cylindricity and flatness of the rotor bearing surfaces are required to be 2 µm. Additionally, the cylindrical nature of the rotor requires that some air pads are perpendicular to each other, and therefore a tolerance of 2 µm is also applied on the perpendicularity of the rotor bearing surfaces, as depicted in Fig. 2.

Another critical point is material selection when producing a device capable of performing measurements with microscale uncertainties while fitting with the requirements of the PACMAN project. The following requirements were considered during the material selection process for the SESHAT's rotor:

- A final form error of < 2 µm
- A final surface roughness Ra of < 0.4 µm
- A non-ferromagnetic material
- Coefficient of thermal expansion as close as possible to alumina's ($7.2 \times 10^{-6}\ K^{-1}$)
- Low density: final rotor weight requirement < 0.5 kg
- High stiffness: final rotor stiffness > 100 N/µm
- The possibility to be open without becoming out of tolerances

The piezo motor leading the rotor requires the hardness of alumina ceramic. For this reason, a ring will be bounded to the rotor whose material should have a thermal expansion coefficient close to the one of alumina in order to prevent bi-material deformations during temperature fluctuations. The air bearing is composed of 12 air pads opposite each other and applying about 200 N of force for a couple of the larger ones and 50 N for the smaller ones. The rotor deformation under the pressure applied when the air is switched on should remain at a micrometric level, which requires high stiffness.

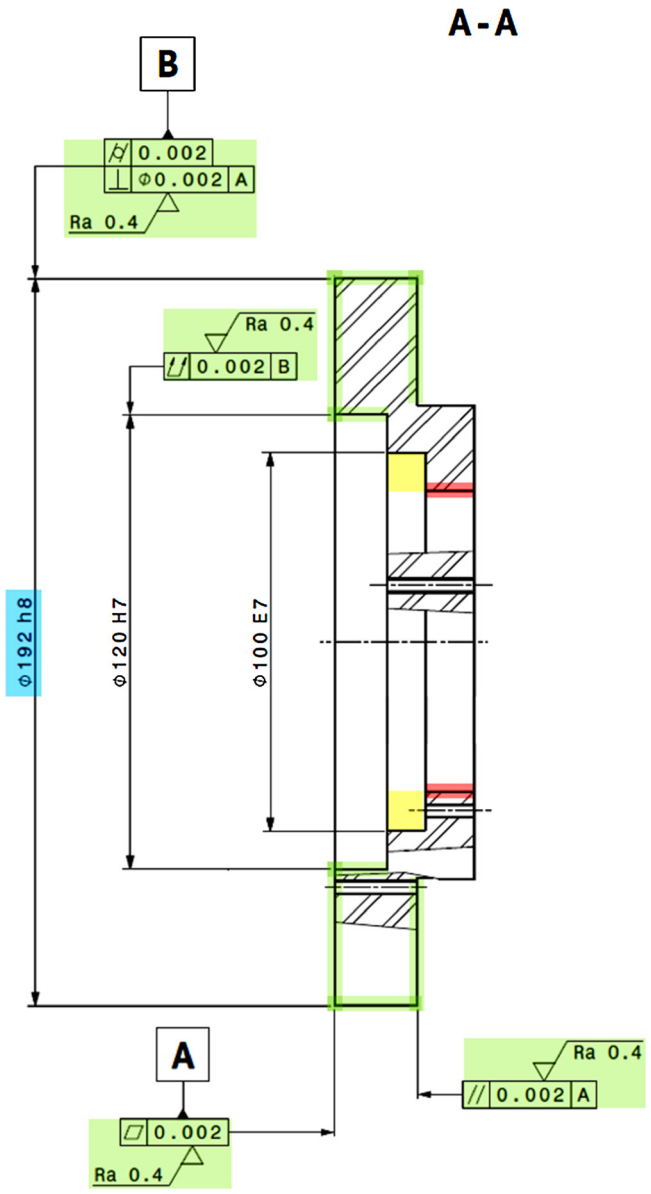

Fig. 2. Technical drawing of the rotor showing the 2 µm tolerances required from the air pads (green) and the largest dimension (192 mm – blue). The location of the ceramic ring (required for successful use of the piezo motor) is highlighted in yellow while the open surface required for powder removal is in red.

Ti-6Al-4 V is a stiff alloy compatible with the different requirements but the weight limit for a plain rotor, despite its relatively low density of 4.42 kg/dm^3. Nevertheless, it is suited for additive manufacturing and shows interesting properties after Selective Laser Melting (SLM) [7–11]. Bordin et al. have recently demonstrated that Ti-6Al-4 V can be

turned to reach the roughness required for the SESHAT rotor [12]. Taking this into account and in order to meet the 1.2 kg weight limit for the sensor system (0.5 kg for the rotor), the decision was made to manufacture it by SLM. A concern with this technique, affecting its suitability for this application, was the lack of accurate prediction of the residual stress in Ti-6Al-4 V (affecting the move during notch cutting). According to Yadroitsev and Yadroitsava's paper, which gathers results from different studies, they observed that the stress is higher along the direction of the laser path than in the perpendicular direction and that it increases with the number of layers, but the amount of stress is varying much with the thickness, which makes it barely possible to predict [13]. Nevertheless, these results were confirmed and balanced by the observations reported later by Mishurova et al. who added that the stress releasing treatment relieves the residual stresses created by SLM [14]. According to this statement, the rotor stresses should be mainly due to the long-known residual stresses due to the machining process, particularly as they affect thin parts more [15]. Additionally, unlike regarding roughness after SLM and manufacturing [16,17], there was insufficient information in the literature concerning achievements on shape quality. Consequently best suited manufacturing techniques on thin samples obtained by SLM are not well documented either, although information can be found concerning turning a 12.5 mm thick hollow cylinder [18], thinner parts were not studied. These observations led to the tests on 1.5 mm and 2 mm thick walls presented in the following chapters.

This article presents the development and optimisation of a test rotor obtained by Selective Laser Melting (SLM) aiming to meet the tolerances required for the SESHAT. The potential of precision machining as well as the impact of stress relief and associated deformation were investigated and are presented.

Acronyms used in this document:

- CLIC Compact Linear Collider
- EDMElectron Discharge Machining
- PACMAN Particle Accelerator Component's Metrology and Alignment to the Nanometre scale
- SESHAT Shape Evaluating Sensor: High Accuracy and Touchless
- SLM Selective Laser Melting

2. Design of the rotor for selective laser melting (SLM)

After the motivations for the choice of Ti-6Al-4 V were detailed in the introduction, the different steps toward the finished rotor are detailed in this section:

- Design for SLM of the rotor
- Heat treatment
- Grinding vs Turning
- Notch cutting

2.1. Design adapted to selective laser melting (SLM)

A technical drawing for a metallic rotor was produced based on the design requirements of the SESHAT, as depicted in Fig. 2. In order to facilitate effective SLM, an external wall was left open to enable powder removal after manufacture. During manufacture, the complete form (without the presence of the holes or the notch) was produced. An additional thickness was added to the walls in order to facilitate later machining, threading and cutting. For components showing no bulk distortion, 0.5 mm additional thickness is known to be sufficient to enable effective material removal through traditional machining. During SLM, when the laser beam melts a large amount of matter in a single layer, there is a significant amount of heat dissipation in neighbouring regions which induces residual stresses or distortions, as discussed in the introduction. To minimise the effect of these, the rotors were manufactured at a build angle of 6° between the support and the part, and the orientation of the notch was set perpendicular to the laser path, which was as symmetric as possible with respect to the notch plane. This small built angle required the production of supports within the sample as shown in Fig. 3.

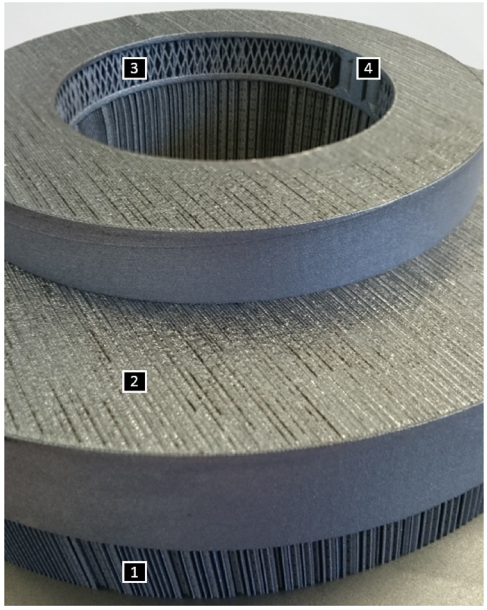

Fig. 3. TiAl6V4 rotor version 1 out of the SLM. The structures required to support the bottom surface of the rotor are shown (1). The surface pattern reflects the staircase effect associated with the low inclination surface of SLM (2). The internal structures of the rotor is an array of rhombuses (3). At the location of holes and the rotor notch, the part is solid (4).

2.2. Additive manufacturing

The rotors were manufactured with a SLM 280 H L form SLM Solutions. This system features a 400 W ytterbium continuous wave fibre laser operating at a wavelength of 1070 nm and a 3 axis scanning system. The build envelope is 280 × 280 × 365 mm^3 reduced by the build plate thickness. The layer thickness was 50 µm and the platform temperature was 200 °C. The laser beam diameter has been measured at 77 u m at beam waist location in accordance with EN ISO 11146-2. The process chamber was inerted with an argon flow at a speed of 6.2 m/s (measured in the piping leading to the vacuum pump) and an overpressure of 12 mbar. The argon has a purity grade of 4.6 (99.996 %). The process parameters were set at a volumetric energy density of 60.3 J/mm^3 with a laser beam power of 275 W and a scan speed of 760 mm/s. These parameters were qualified for the manufacturing of Helium leak tight parts with densities above 99.95 %.

2.3. Heat treatment

The rotors were heat-treated at 650 °C for 2 h in a vacuum furnace with a subsequent cooling under vacuum to 100 °C. Below this temperature, the parts were air cooled. Heat treatment was performed before removing the supports to the titanium base plate on which the samples were manufactured, as shown in Fig. 4.

2.4. Grinding and turning of the part

Two types of machining were compared: turning and grinding. The motivation for this choice is that these traditional techniques are known to achieve excellent results on parts featuring an axis of symmetry, while no report was found in the literature on what was the best-suited technique to be applied on SLM part, and, more generally, parts created

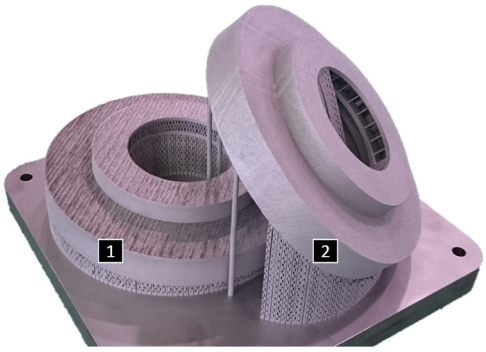

Fig. 4. Rotor version 2 (1) was printed simultaneously with a spare part (2) in order to save handling time.

by additive manufacturing and aiming to reach micrometric tolerances on the form. The machining was performed by initially generating a reference surface, then holding the part in place, and it was based on water coolant.

The trials were made on a Studer S20 from 1991. The outer cylinder was machined with a soft grinding wheel with a size of Ø 350 × 25 × 127 mm (diameter × thickness × central bore) and thin alumina grains arranged in an open structure (57 A 80 J 7 V300 W). Another soft grinding wheel with the same size and thinner silicon carbide grains with a medium structure (15C 120 H 5 V035 W) was then used, reaching the final performances. Concerning the inner cylinder, the tests were performed with two grinding wheels with diameters of 60 mm and 80 mm and with thin and thinner silicon carbide grains arranged in a medium and very open structure respectively (Ø 60 mm, 57C 80 L 5 V53; Ø 80 mm 57C 100 G 13 V53). The lowest speed of 1600 rpm was chosen for the wheels and 80 rpm for the work head.

For turning, the full rotor was held in a NAKAMURA-TOME SC-250 lathe from 2012, equipped with a cutting insert for titanium. As little force as possible was applied by the chuck to hold the rotor. The external cylinder, the face and the internal cylinder were all turned without unmounting the part.

2.5. Electron discharge machining of the notch

Electron Discharge Machining (EDM) was used to notch the rotor. A 0.25 mm diameter wire was used to cut the part at a speed of 33 µm/s. Cooling was performed using deionised water.

3. Results

3.1. Selective laser melting (SLM)

3.1.1. Rotor version 1

The first version of the rotor is shown in Fig. 3. Despite being designed oversized, after manufacture, sample version 1 was found to be elliptical such that its semi-minor axis, aligned with the built direction and perpendicular to the laser path, was 1.2 mm smaller than the nominal rotor dimension. For this reason, it was decided that the sample version 1 would be used to optimise the machining parameters:

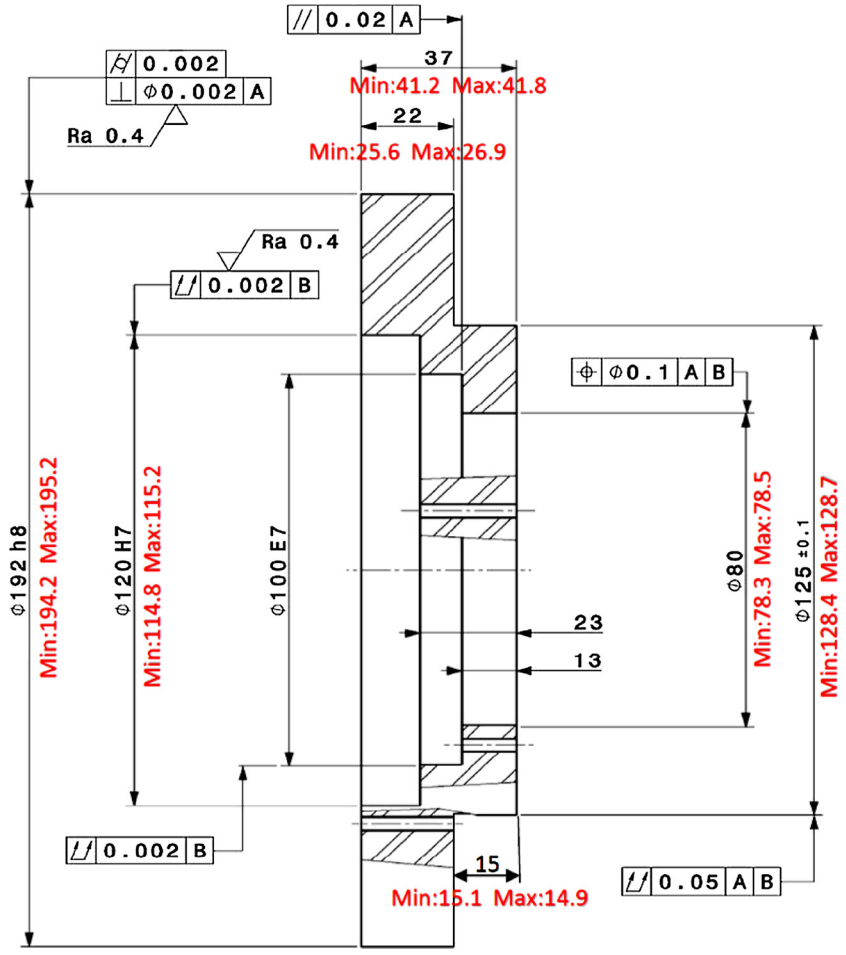

Fig. 5. Measurements after Selective Laser Melting of the second version, showing the range of the lengths variations [mm]. The nominal values are the ones of the rotor in its final version, namely after machining.

to identify the most suitable grinding medium and machining technique for this application.

3.1.2. Rotor version 2

For the second version of the rotor, the oversizing of the external walls was extended to 2 mm. This increased the amount of deposited material thus the residual stresses and manufacture time for the part, however, was performed in order to reduce the likelihood of unsuccessful machining. After manufacture, some cracking were observed in the support structure of this sample, nevertheless, this was found to have a minimal impact on the global orientation of the sample and the relative build direction. The result appears in Fig. 4. The second version of the rotor was found to show similar magnitude elliptical distortions with the same orientation as sample version 1 (of up to 1.1 mm). The range of the results appear in Fig. 5. Additionally, we can observe that the distortions resulting from the manufacturing do not appear regular nor proportional to the built thickness. Nonetheless, the increased oversizing of this version of the part was such that there was sufficient material within the deposited rotor to allow the sample to be machined to its nominal dimensions.

3.1.3. Other considerations

This study is not focused on the thorough evaluation of the quality of the part obtained by SLM. Indeed, previous tests performed with the same SLM 280 H l showed that the density of the resulting titanium was 99.97 % and confirmed that the residual stresses were removed after heat treatment, so we considered these characteristics for granted.

The measurements with the results after SLM, reported in Fig. 5, were performed with a calliper. The form deviations after grinding, turning and notch cutting, reported in Table 1, were measured with a Leitz Infinity CMM with a $MPE_E = 0.3\,\mu m + L/1000\,\mu m$ (with the length L in millimetres). The visual measurements results shown in Fig. 8 were obtained with an O-Inspect with a $MPE_E = 1.9\,\mu m + L/300\,\mu m$ (with the length L in millimetres).

3.2. Grinding and turning of the part

The thin workpiece was not cooling down in the same way as a plain titanium part would: the heat, which could not diffuse in the depth of the material, was affecting the grinding by melting and burning the titanium alloy at the surface. Additionally, the excess thickness of the SLM rotor walls was not consistent and resulted in changes in behaviour as a function of the angular position. A deposition of titanium on the grinding wheel was affecting the work. The coolant was injected either on the outer part or in the rotor opening to enable the grinding, as can be observed in Fig. 6, nevertheless, the wheel had to be often reground. The soft grinding wheel with thinner silicon carbide grains used afterwards reduced the deposition without eliminating it, bringing the better results reported in Table 1.

The results on the cylindricity, perpendicularity and planarity obtained on the external surfaces after grinding were approaching the very demanding 2 µm tolerances (see Table 1). Nevertheless, by design of the machine, the spinning speed of the wheel has a lower limit. This limit was reached while machining the inner cylinder. As a result, the titanium part was heating up such that not only the surface was burning, but also the whole workpiece was getting distorted. Consequently, the tolerances could never be approached on the whole part and the idea of grinding the rotor was dropped.

After turning, the accuracy reached on the test part was not as excellent due to a conicity affecting the flatness at the micrometric level, but stayed within reasonable values, and all the faces could be done, as reported in Table 1. On the second part, the flatness meets the 2 µm tolerance. The first part was lighter than expected, probably due to the sub-millimetre thin walls in some places. The results obtained on the final rotor were better than on the test version, as written in Table 1, but the part was heavier.

3.3. Notch cutting

After the manufacture of the version 2 rotor, the test rotor version 1 was opened in order to observe the amplitude of the deformations dues to the residual stresses probably introduced during machining. The notch appears in Fig. 7. Despite the symmetry introduced in the design, the notch perpendicular to the laser path and the stress releasing heat treatment which must have almost eliminated the residual stresses, the machining, most probably the grinding, induced non-negligible residual stresses. Indeed, the cutting process moved the rotor's flat surface from a conical form error of a few microns to an asymmetrical form error larger than two tens of microns, as pictured in Fig. 8. However, the external cylinder form error was increased by a couple of microns only, which is encouraging for who may work with a requirement on the cylindricity only.

As a result, the rotor's surfaces were out of the acceptable limits of 5 µm and therefore could not be used for the SESHAT. The notch cutting of the rotor version 2 may be performed as the completion step of the SESHAT when all the other elements will be properly assembled and operational, or the device may be kept as an additional rotary measurement system, without the opening. As turning heats less than grinding, the stress release is expected to have a smaller impact on the form errors.

Table 1
Recapitulation of the results obtained on the different versions of the rotors before and after machining and cutting. The tolerance on the cylindricity, perpendicularity, parallelism and flatness was 2.

	Version 1	Version 2
Nominal wall thickness + excess	*1 mm + 0.5 mm*	*1 mm + 1 mm*
After SLM	Elliptic shape with semi-minor axis < nominal	Acceptable distortions
	Support structure intact	Broken support structure
Use	Tests and tuning	Composes the SESHAT
During grinding	Surfaces were burning, cylinder ∅120 distorted	–
After grinding	Cylindricity ∅192: 3 µm	–
	Perpendicularity of bearing surfaces: 2 µm	–
	Flatness of bearing surfaces: 5 µm	–
After turning	Cylindricity ∅192: 4 µm	Cylindricity ∅192: 3.8 µm
	Cylindricity ∅120: 7 µm	Cylindricity ∅120: 6.7 µm
	Perpendicularity of bearing surfaces: 10 µm	Perpendicularity of bearing surfaces: 2.5 µm
	Parallelism of bearing surfaces: 5 µm	Parallelism of bearing surfaces: 2 µm
	Flatness of bearing surfaces: 7 µm	Flatness of bearing surfaces: 2 µm
After EDM notch cutting	Cylindricity ∅192: 6 µm	–
	Flatness of bearing surfaces: 25 µm	–
Weight after machining	357 g	450 g

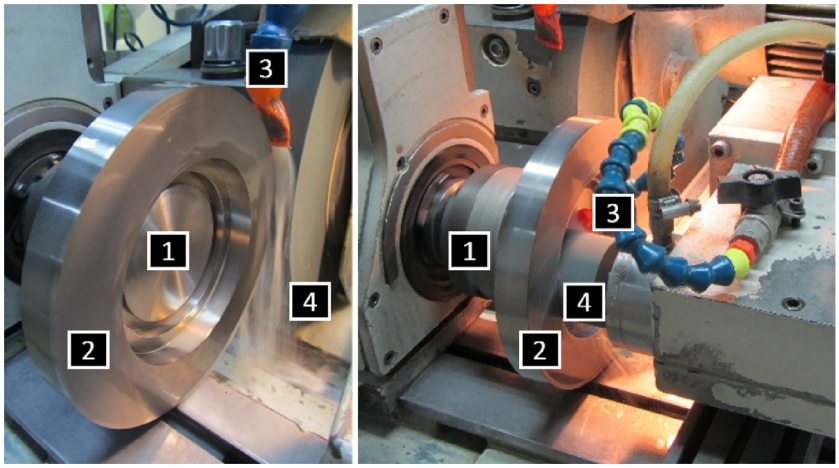

Fig. 6. Grinding of the titanium rotor version 1. The chuck (1), the rotor (2) and the grinding wheel (3) are shown, along with the coolant (4) which was applied externally or internally.

Fig. 7. Rotor type A, first version, after turning and notch cutting.

4. Discussion

High precision machining is the base for high precision mechanics, itself the base for high precision measurement systems. Taking into account the machining of the parts used for a high precision system is an important step of its design. The tolerances of 2 µm were meaningful as they are the nominal tolerances for the porous air pads adjusted to the bearing surfaces. Nevertheless, expecting the state of the art machining to reach these tolerances without problems on such a part would have been unrealistic. Furthermore, the prediction of the stresses introduced in the SLM part is not accurate enough to foresee the behaviour of such a part after notch cutting. The results obtained in this study showed that a lightweight stiff rotor could be manufactured and turned to a stage which makes it usable by a high precision air bearing - diminishing nevertheless the quality of the bearing which will require software corrections (mapping) and radial stiffness reduction by increase of the air gaps - and that the cylindricity of a part open in the

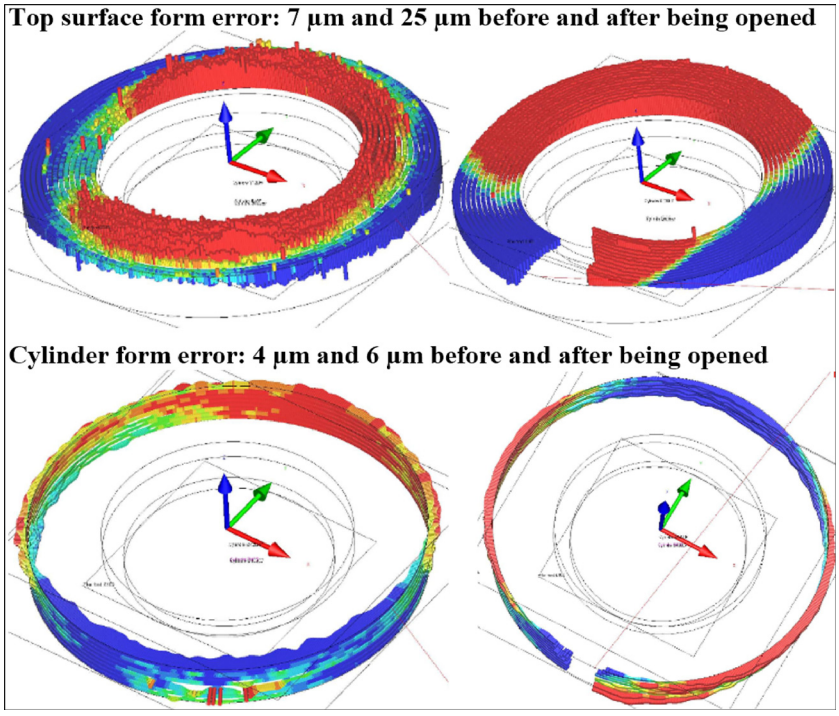

Fig. 8. Rotor form measurements before and after being opened.

radial direction was affected at the micrometric level.

5. Summary

The concept of the Shape Evaluating Sensor: High Accuracy and Touchless is based on a lightweight air bearing with tolerances of 2 µm on the rotor's bearing surfaces which feature a notch in the radial direction. In order to aim to their achievement, the choice was made to manufacture the rotor in Ti-6Al-4 V titanium alloy by Selective Laser Melting and turn it at best.

The oversized dimensions applied to the first SLM adapted technical drawing were not sufficient, which led to actual dimensions smaller than the nominal ones before starting the finishing process. This was taken into account for the design of the new parts: one similar to the first one which was turned, and a second one printed at 45° meant to be a spare part.

The first distorted part was used as a test part for the machining: the thin walls of the outer cylinder brought problems of heat transfer during grinding which led to the melting of the titanium alloy and the alteration of the grinding wheel properties. On the inner cylinder, these were added to the speed limitation of the grinding machine and led to a distortion of the entire part. As a result, an SLM part can be ground to cylindricity, perpendicularity and flatness better than 5 µm on the outer cylinder and faces.

Turning was the solution suiting better the inner cylinder: the results obtained by turning on the final part were 2 µm of flatness and 7 µm of cylindricity for the most challenging faces.

The opening of the test part engendered axial distortions adding 18 µm to the flatness and radial distortions adding 2 µm to the cylindricity. A part with such distortions could not be used for the SESHAT, as a result, the study of the sensor will be continued with a non-opened rotor.

A release of the constraints containing the residual stresses from grinding and turning in a part with the SESHAT rotor's shape engenders a move of the surfaces affecting the cylindricity at the micrometric level and the flatness by a couple of tens of microns.

6. Conclusion and future work

Machining techniques relying on heat diffusion in the material ought to be very carefully considered when applied to parts produced by Selective Laser Melting with thin walls for high precision applications and the cooling procedure needs to be optimised. To that end, tests could be performed to assess which shape would fit better the inner walls in order to optimise the cooling.

Residual stresses after machining is a topic widely covered by the literature and the conclusions stay valid for machining a part obtained by additive manufacturing: to reduce the residual stresses after machining one should perform the rough machining and heat treat the part before the completion of the work. Nevertheless, it seems that the residual stresses within the rotor affect more the flatness than the cylindricity.

Acknowledgements

The European citizens who supported this work through European Union's 7th Framework Programme Marie Skłodowska-Curie actions (grant agreement PITN-GA-2013-606839) and the European Organisation for Nuclear Research.

The AMC-Technologies business partners who accepted the challenge of this test project.

The CERN colleagues providing their best-suited technologies and methodologies or sharing their ideas about how to accomplish this work. Particularly, François Morel for the design of the parts and the metrology group for their accurate measurements.

References

[1] E. Sachs, M. Cima, J. Cornie, D. Brancazio, J. Bredt, A. Curodeau, T. Fan, S. Khanuja, A. Lauder, J. Lee, S. Michaels, Three-dimensional printing: the physics and Implications of additive manufacturing, CIRP Ann. - Manuf. Technol (1993) 257–260 42/1/1993.

[2] M. Aicheler (Ed.), A Multi-TeV Linear Collider Based on CLIC Technology: CLIC Conceptual Design Report, CERN, Geneva, 2012.

[3] D. Caiazza, N. Catalan Lasheras, H. Mainaud Durand, M. Modena, C. Sanz, D. Tshilumba, V. Vlachakis, M. Wendt, S. Zorzetti, New solution for the high accuracy alignment of accelerator components, Phys. Rev. Accel. Beams. 20 (2017), https://doi.org/10.1103/PhysRevAccelBeams.20.083501.

[4] L. Bottura, M. Buzio, S. Pauletta, N. Smirnov, Measurement of magnetic axis in accelerator magnets: critical comparison of methods and instruments, Instrum. Meas. Technol. Conf. (2006) 765–770 (Accessed 23 January 2017), http://ieeexplore.ieee.org/abstract/document/4124432/.

[5] D. Caiazza, P. Arpaia, C. Petrone, S. Russenschuck, Performances of the stretched - and vibrating - wire techniques and correction of background fields in locating quadrupole magnetic axes, XXI IMEKO World Congr. (2015).

[6] N. Galindo Munoz, N. Catalan Lasheras, S. Zorzetti, M. Wendt, A. Faus Golfe, V. Boria Esbert, ELECTROMAGNETIC FIELD PRE-ALIGNMENT OF THE COMPACT LINEAR COLLIDER (CLIC) ACCELERATING STRUCTURE WITH HELP OF WAKEFIELD MONITOR SIGNALS, Proc. IBIC 2015 (2015) (Accessed 23 January 2017), https://accelconf.web.cern.ch/AccelConf/IBIC2015/papers/tupb054.pdf.

[7] B. Dutta, F.H.(Sam) Froes, The additive manufacturin (AM) of titanium alloys, Met. Powder Rep. 72 (2017) 96–106.

[8] H. Rafi, N. Karthik, H. Gong, T. Starr, B.E. Stucker, Microstructures and mechanical properties of Ti6Al4V parts fabricated by selective laser melting and electron beam melting, J. Mater. Eng. Perform. 22 (2013) 3872–3883.

[9] P. Krakhmalev, G. Fredriksson, I. Yadroitsava, N. Kazantseva, A. du Plessis, I. Yadroitsev, Deformation behavior and microstructure of Ti6Al4V manufactured by SLM, Phys. Procedia 83 (2016) 778–788, https://doi.org/10.1016/j.phpro.2016.08.080.

[10] E. Wycisk, C. Emmelmann, S. Siddique, F. Walther, High cycle fatigue (HCF) performance of Ti-6Al-4V alloy processed by selective laser melting, Adv. Mater. Res. 816–817 (2013) 134–139.

[11] X. Zhao, S. Li, M. Zhang, Y. Liu, T.B. Sercombe, S. Wang, Y. Hao, R. Yang, L.E. Murr, Comparison of the microstructures and mechanical properties of Ti-6Al-4V fabricated by selective laser melting and electron beam melting, Mater. Des. 95 (2016) 21–31.

[12] A. Bordin, S. Sartori, S. Bruschi, A. Ghiotti, Experimental investigation on the feasibility of dry and cryogenic machining as sustainable strategies when turning Ti6Al4V produced by additive manufacturing, J. Clean. Prod. 142 (2017) 4142–4151, https://doi.org/10.1016/j.jclepro.2016.09.209.

[13] I. Yadroitsev, I. Yadroitsava, Evaluation of residual stress in stainless steel 316L and Ti6Al4V samples produced by selective laser melting, Virtual Phys. Prototyp. 10 (2015) 67–76, https://doi.org/10.1080/17452759.2015.1026045.

[14] T. Mishurova, S. Cabeza, K. Artzt, J. Haubrich, M. Klaus, C. Genzel, G. Requena, G. Bruno, An assessment of subsurface residual stress analysis in SLM Ti-6Al-4V, Materials. (2017) 10, https://doi.org/10.3390/ma10040348.

[15] E. Brinksmeier, J.T. Cammett, W. König, P. Leskovar, J. Peters, H.K. Tönshoff, Residual stresses—measurement and causes in machining processes, CIRP Ann.-Manuf. Technol. 31 (1982) 491–510.

[16] B. Vayssette, N. Saintier, C. Brugger, M. Elmay, E. Pessard, Surface roughness of Ti-6Al-4V parts obtained by SLM and EBM: effect on the high cycle fatigue life, Procedia Eng. 213 (2018) 89–97, https://doi.org/10.1016/j.proeng.2018.02.010.

[17] M. Shunmugavel, A. Polishetty, M. Goldberg, R. Singh, G. Littlefair, A comparative study of mechanical properties and machinability of wrought and additive manufactured (selective laser melting) titanium alloy – Ti-6Al-4V, Rapid Prototyp. J. 23 (2017) 1051–1056, https://doi.org/10.1108/RPJ-08-2015-0105.

[18] M. Shunmugavel, A. Polishetty, M. Goldberg, R.P. Singh, G. Littlefair, Tool wear and surface integrity analysis of machined heat treated selective laser melted Ti-6Al-4V, Int. J. Mater. Form. Mach. Process 3 (2016).